NEW OCEAN WINDS SATELLITE MISSION TO PROBE HURRICANES AND TROPICAL CONVECTION

BY CHRISTOPHER S. RUF, ROBERT ATLAS, PAUL S. CHANG, MARIA PAOLA CLARIZIA, JAMES L. GARRISON, SCOTT GLEASON, STEPHEN J. KATZBERG, ZORANA JELENAK, JOEL T. JOHNSON, SHARANYA J. MAJUMDAR, ANDREW O'BRIEN, DEREK J. POSSELT, AARON J. RIDLEY, RANDALL J. ROSE, AND VALERY U. ZAVOROTNY

The CYGNSS constellation of eight satellites, scheduled to launch in 2016, will measure hurricane-force ocean-surface wind speed in the presence of precipitation encountered in the inner core of hurricanes.

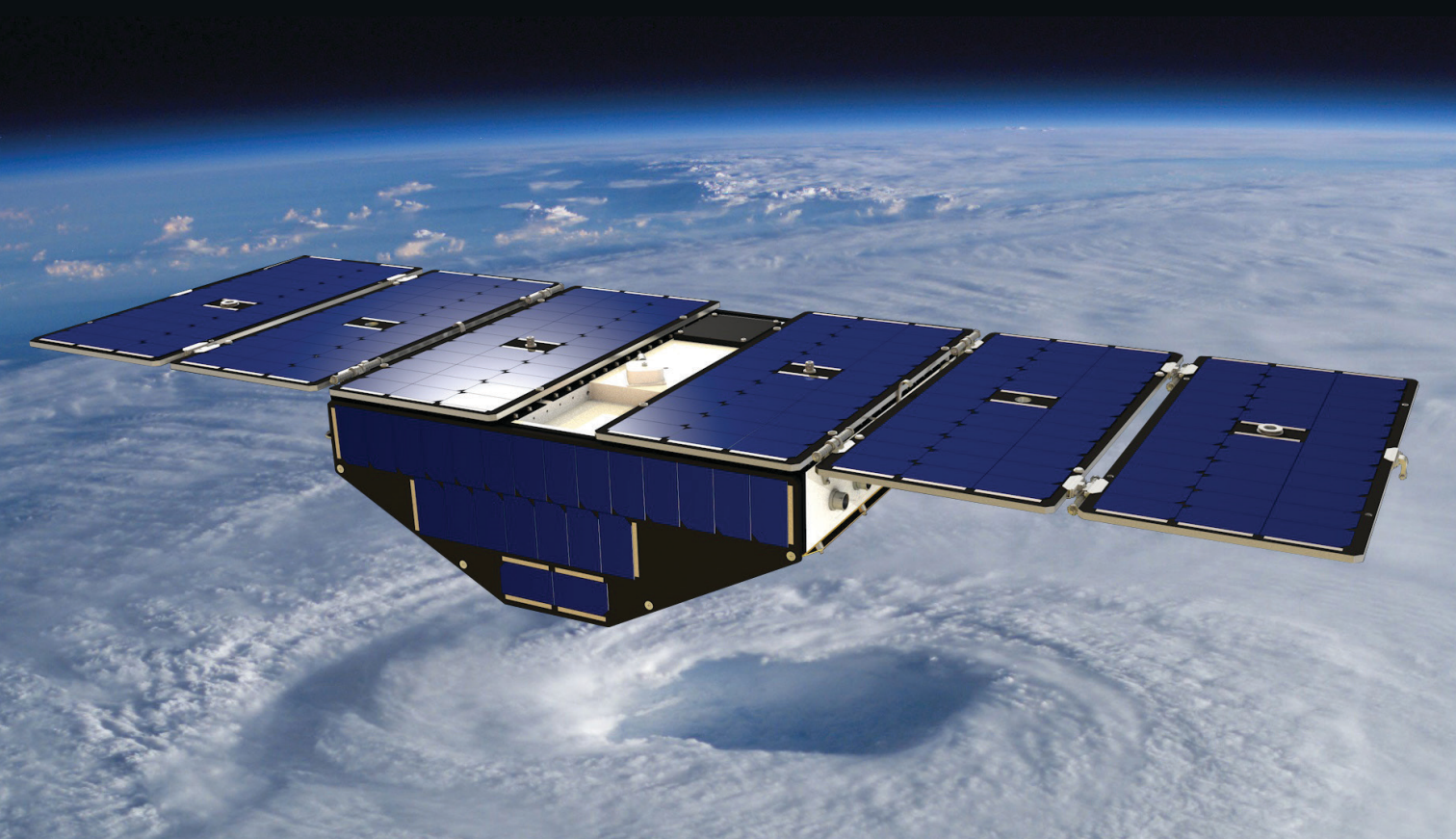

The Cyclone Global Navigation Satellite System (CYGNSS) is a constellation of eight small satellites designed to measure ocean surface wind speed with high temporal resolution, 25-km spatial resolution, and extensive spatial coverage, under all precipitating conditions and over the full dynamic range of wind speeds experienced in a tropical cyclone (TC). Near-surface winds over the ocean are major contributors to and indicators of momentum and energy fluxes at the air–sea interface. The mission's goal is to better understand the coupling between surface winds and the moist atmosphere within a TC. CYGNSS will provide surface winds in the TC inner core, including regions beneath the eyewall and rainbands that could not previously be measured from space owing to attenuation and scattering by the rain and ice aloft. Mission simulation studies predict typical revisit times in hours, which is a dramatic improvement over multiple-day revisit times obtained with individual spaceborne scatterometers. The CYGNSS wind fields, when combined with precipitation fields sampled as frequently [e.g., as produced by the Global Precipitation Measurement (GPM) core satellite and its constellation of precipitation imagers], will map the evolution of both the precipitation and underlying wind fields throughout complete TC life cycles. Together, they will provide coupled observations of moist atmospheric thermodynamics and ocean surface response, enabling new insights into TC inner-core dynamics and energetics.

AFFILIATIONS: Ruf, Clarizia, Posselt, and Ridley—University of Michigan, Ann Arbor, Michigan; Atlas—NOAA/AOML, Miami, Florida; Chang and Jelenak—NOAA/NESDIS/STAR, College Park, Maryland; Garrison—Purdue University, West Lafayette, Indiana; Gleason and Rose—Southwest Research Institute, Boulder, Colorado; Katzberg*—NASA LaRC, Hampton, Virginia; Johnson and O'brien—The Ohio State University, Columbus, Ohio; Majumdar—University of Miami, Coral Gables, Florida; Zavorotny—NOAA/ESRL, Boulder, Colorado
* Retired
CORRESPONDING AUTHOR: Prof. Christopher Ruf, Dept. of Climate and Space, University of Michigan, 2455 Hayward St., Ann Arbor, MI 48109-2143
E-mail: cruf@umich.edu

The abstract for this article can be found in this issue, following the table of contents.

DOI:10.1175/BAMS-D-14-00218.1
A supplement to this article is available online (10.1175/BAMS-D-14-00218.2)

In final form 31 May 2015

SCIENTIFIC MOTIVATION. TC track forecasts have improved in accuracy by approximately 50% since 1990, largely as a result of improved mesoscale and synoptic modeling and data assimilation. During the same period, improvements in intensity forecasting have been relatively modest, although recent advances in high-resolution modeling have shown promise (Gall et al. 2013). The lack of improvement in intensity forecast skill has, in part, resulted from inadequate observations and modeling of the inner core of the storm. Observations of the inner core by the current suite of spaceborne remote sensing instruments tend to be obscured by the intense precipitation found in the eyewall and inner rainbands. In addition, the current suite of polar-orbiting instruments tends to inadequately sample the shorter time-scale stages of the TC life cycle such as rapid intensification.

The value of wind observations in precipitating conditions. In addition to the rainbands and eyewall of tropical cyclones, precipitation-producing tropical deep convection exhibits organization on a wide range of spatial and temporal scales. In particular, mesoscale convective systems (MCSs) contribute more than half of the total rainfall in the tropics (Rickenbach and Rutledge 1998; Nesbitt et al. 2000) and serve as the precursors to TCs (Houze 2004, and references therein). MCSs are affected by feedback on the sensible and latent heat fluxes at the ocean surface, as well as on their structure and propagation velocity. Over the ocean, the organization of the fluxes depends on a complex interaction between surface-level winds and storm dynamics (Houze 2004). MCS development and characteristics depend critically on the interaction between ocean surface properties, moist atmospheric thermodynamics, radiation, and convective dynamics (Stephens et al. 2004). In addition to producing the bulk of the rainfall in the tropics, MCSs also play a key role in the formation and propagation of the Madden–Julian oscillation (MJO), which directly influences the genesis of tropical storms in the Pacific Ocean and Caribbean Sea.

Understanding MJO structure and improving its forecasting require detailed knowledge of the convective environment. Existing measurement systems are capable of characterizing the thermodynamic environment and rain rate associated with the MJO, but information about the surface winds has been limited. Conventional satellite scatterometer measurements are capable of observing the frequency and characteristics of the MJO, but their effectiveness is significantly reduced by their inability to observe surface-level winds in heavy precipitation (Arguez

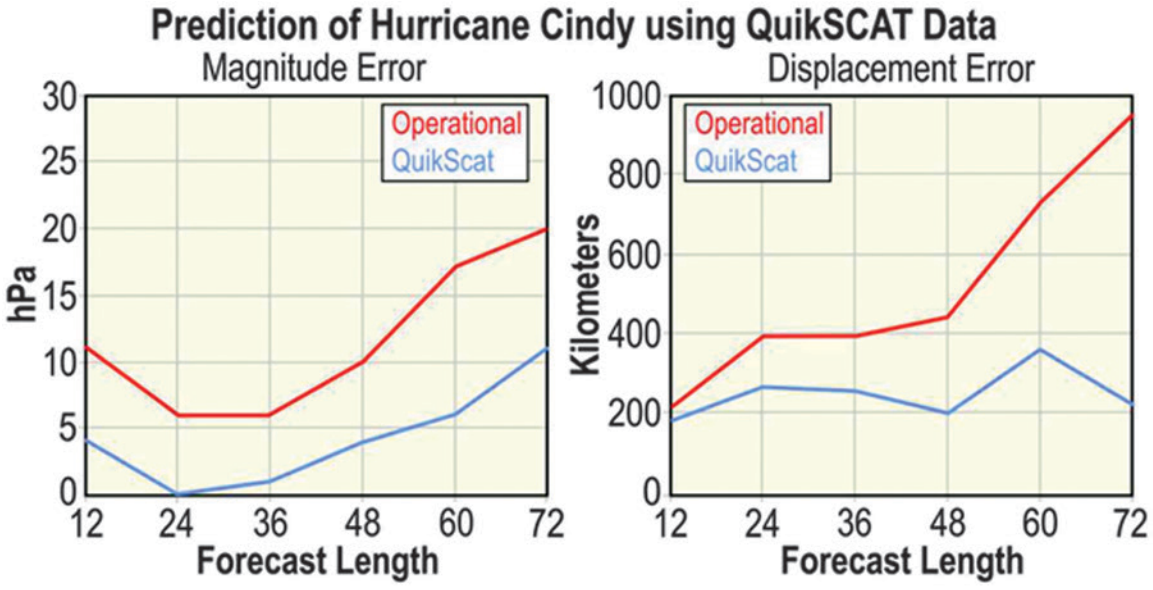

Fig. 1. Hurricane Cindy case study of the impact of satellite wind field observations on (left) intensity and (right) position forecast error (Atlas et al. 2005a). Both forecasts use the NCEP operational data assimilation system and forecast model in place at the time of the study. The "operational" run used all ground-based and satellite data that were assimilated operationally, including satellite atmospheric sounders but not QuikSCAT surface winds. The "QuikSCAT" run used all operational data plus the QuikSCAT surface winds. Neither run used any bogus data or vortex relocation. This case demonstrates the potential for satellite surface wind data to improve TC predictions, but it does not imply that this level of improvement would occur in all cases.

et al. 2005). The limitations of existing spaceborne measurements of ocean surface winds under precipitating conditions become even more severe in TCs. As a result, in the absence of reconnaissance aircraft, the availability and accuracy of wind speed estimates in the TC inner core are often highly compromised. For example, errors in operational estimates of intensity using the Dvorak technique are over 2.5 m s^{-1} in about half of all cases and over 6 m s^{-1} in a quarter of all cases. Large outliers in intensity estimation error also exist (Brown and Franklin 2004).

The value of frequent wind observations. Most current spaceborne active and passive microwave instruments are in polar low-Earth orbits (LEOs). The orbits maximize global coverage but can result in large gaps in the tropics. Schlax et al. (2001) present a comprehensive analysis of the sampling characteristics of conventional polar-orbiting swath-based imaging systems, including consideration of so-called tandem missions. The study demonstrates that a single broad-swath, high-resolution scatterometer system cannot resolve synoptic-scale spatial detail everywhere on the globe, and in particular not in the tropics. The irregular and infrequent revisit times (typically 11–35 h) are likewise not sufficient to resolve synoptic-scale temporal variability. Missed sampling of an organized storm system can occur when it passes through an imager's coverage gap or when its motion is offset from the motion of the imager's swath.

The value of wind observations for tropical cyclone forecasting. Observations of sea surface winds, waves, and rain-rate conditions are among the most important factors in both improving our understanding of TCs and predicting them operationally. Climatologists, oceanographers, and operational forecasters use wind information principally in three ways: 1) to improve fundamental knowledge about atmospheric phenomena, such as El Niño, TCs, and large-scale tropical oscillations; 2) to provide input forcing for deterministic models of the coupled ocean–atmosphere system; and 3) to improve the accuracy and reliability of, and to extend the lead time for, forecasts of TCs (Atlas et al. 2001, 2005b).

A case of strong positive impact of satellite wind observations on TC forecast skill is illustrated by the 60-h forecast of Hurricane Cindy that had been performed with an earlier version of the National Centers for Environmental Prediction (NCEP) operational system, with and without QuikSCAT wind fields (Atlas et al. 2005a). Errors in the forecast of storm intensity and track are shown in Fig. 1. The intensity forecast error (error in forecasting the maximum air

pressure depression in the TC core) is reduced by approximately 50% or more with QuikSCAT for all forecast lengths. The track forecast error (error in forecasting the location of the TC eye) also grows much more slowly with forecast length when wind field data are included, reaching approximately 200-km error at 72 h as opposed to approximately 1000 km when no satellite data are included. This case is one example of the potential that satellite surface wind data have to improve tropical cyclone predictions, but this level of improvement does not occur in all cases.

GNSS BISTATIC SCATTEROMETRY. The CYGNSS mission uses a bistatic radar method (i.e., transmitter and receiver in different locations) for measuring winds, as opposed to the monostatic method (i.e., transmitter and receiver on the same satellite) used by traditional scatterometers. The use of satellite navigation signals as the transmitter half of a bistatic radar for Earth remote sensing is commonly referred to as Global Navigation Satellite System reflectometry (GNSS-R). There are a number of navigation satellite systems currently in operation, the most common being the global positioning system (GPS). The GNSS-R technique benefits from significantly reduced sensor requirements as compared to traditional scatterometers, since no transmitter is required on the "receive only" spacecraft.

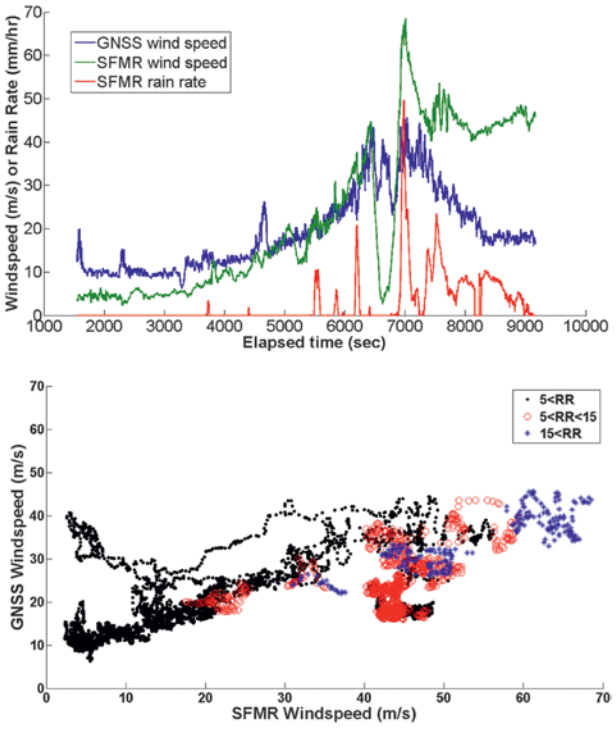

Fig. 2. (top) Time series of the wind speed retrieved by a GNSS-R instrument and by the SFMR during a NOAA P-3 aircraft overpass of Hurricane Bill on 19 Aug 2009. The rain rate retrieved by SFMR is also shown. (bottom) Scatterplot of the GNSS-R- and SFMR-retrieved winds, divided into low, moderate, and heavy rain conditions as determined by the SFMR rain-rate retrieval.

Airborne development of ocean surface wind retrieval by GNSS-R. The first GNSS-R sensor, based on a commercial GPS chipset, was field tested in 1997 over the Chesapeake Bay, collecting GPS signals scattered from the water surface (Garrison et al. 1998). One year later, the relationship between the ocean surface slope probability density and the modulation of the navigation signal caused by scattering from the rough ocean surface was identified, along with the relationship to surface wind speed (Lin et al. 1998). Shortly thereafter, a theoretical framework was developed to characterize the magnitude and spectral and temporal dependencies of the received GNSS signal as functions of the sea state, the measurement geometry, and the signal processing performed by the receiver (Zavorotny and Voronovich 2000). A number of airborne flight campaigns were conducted to continue the study of the sea state–GNSS signal relationship (Garrison et al. 2002).

GNSS-R receivers also began to be deployed on NOAA "hurricane hunter" aircraft to expand the study to very high wind speeds. In 2000, the first GPS-reflected data were acquired inside a TC (Katzberg et al. 2001). Since that time, penetration data inside TCs have been acquired during nearly every Atlantic hurricane season. Wind speed retrievals have been compared to a large set of dropwindsonde data and show the GPS method to be capable of responding well to wind speeds of 40 m s^{-1} or less (Katzberg et al. 2006; Katzberg and Dunion 2009). It should be noted that a small wind direction dependence is likely also present in the data, but it has not yet been fully characterized or incorporated into a retrieval algorithm.

CYGNSS uses the GPS "L1" channel at 1575 MHz (19-cm wavelength), which suffers no appreciable attenuation at even severe rainfall rates. An example of wind speed retrieval in the presence of high rain rates is given in Fig. 2, which shows the wind speed retrieved by a GNSS-R instrument and by the Stepped Frequency Microwave Radiometer (SFMR) during a NOAA P-3 aircraft overpass of Hurricane Bill on 19 August 2009. The rain rate retrieved by SFMR is also shown. SFMR surface observations are directly below the aircraft, with passage through the hurricane eye occurring at elapsed times 6600–6700 s. GNSS-R surface observations are displaced away from

nadir by the specular scattering geometry between the GPS satellite transmitter and the receiver on the aircraft. As such, the two wind measurements are not collocated and a direct comparison between them should not be expected to result in a 1:1 agreement. For example, the transect of the GNSS-R measurements misses the eye during this overpass. A scatterplot of the SFMR and GNSS-R wind speeds is shown in the bottom panel of Fig. 2. It is divided into low, moderate, and heavy rain conditions, as determined by the SFMR rain-rate retrieval, to illustrate that there is no significant difference in the relationship between the two wind speeds as the rain rate varies.

Spaceborne demonstration of ocean surface wind retrieval by GNSS-R. The first successful detection of a GPS-reflected signal in space was reported by Lowe et al. (2002). Subsequently, data from the GPS experiment on the U.K. *Disaster Monitoring Constellation* (UK-DMC) satellite demonstrated that measurements of sufficient signal-to-noise ratio (SNR) could be used to perform successful ocean wave and wind estimation (Gleason et al. 2005, 2010; Clarizia et al. 2009, 2014). These results show that it is possible to detect reflected GPS signals from space across a range of surface wind and wave conditions using a relatively modest instrument configuration. Notably, the UK-DMC sensor had a lower receiver antenna gain (11.8 dBi) and is in a higher orbit (686 km) than the CYGNSS design (14 dBi and 510 km, respectively). Therefore, CYGNSS measurements are expected to have better sensitivity to changes in surface conditions.

The measurements made by a GNSS-R bistatic radar are referred to as delay Doppler maps (DDMs). These are maps of the power in the GNSS signal scattered by the ocean surface after the signals are selectively filtered by time delay and Doppler shift. The time delay is the difference in time of arrival between the direct signal (propagating directly from the transmitting to the receiving satellite) and the signal scattered by the ocean surface. The Doppler shift is the difference in frequency between the signal emitted by the transmitting satellite and the one received from the ocean surface. Both delay and Doppler are varied in the DDM across a range that includes the (delay, Doppler) coordinates of the nominal specular reflection point on the surface with respect to mean sea level. Shorter delays generally correspond to locations above the surface, from which there is no significant scattered signal. Longer delays correspond to isodelay contours on the surface that are centered on the specular point. Doppler values above and below that of the specular point correspond to iso-Doppler contours on the surface to either side of it. The DDM is thus a map of the diffuse surface scattering in the vicinity of the nominal specular point. The transformation between spatial location on the sea surface and location in the DDM is one to one at the DDM specular location, but it can have ambiguities (i.e., multiple spatial locations mapped to the same DDM location) outside the specular region. Examples are shown in Fig. 3 of DDMs measured by the UK-DMC receiver at low, average, and higher wind speed conditions. In each case, the scattered power is highest near the specular point (the top of the "horseshoe" arc in the figure). However, the peak power decreases as the wind speed increases, owing to higher ocean roughness, and the diffuse scattering away from the specular point conversely increases with increasing wind speed and roughness.

Results from the UK-DMC experiment demonstrate a connection between the near-surface wind speed and the measured DDMs. The UK-DMC measurements were made when the specular reflection point passed within 50 km of an active National Data Buoy Center (NDBC) ocean buoy, which provides near-surface (10-m referenced) wind information (Gleason 2013). One example of wind retrieval performance using UK-DMC data is described by Clarizia et al. (2014), in which a minimum variance (MV) wind speed estimator is developed and tested. The estimator is a composite of winds retrieved using five different observables that are derived from the DDMs. Regression-based wind retrievals are developed for each individual observable using empirical geophysical model functions that are derived from NDBC buoy–wind matchups. The root-mean-square (RMS) error in the MV estimator, for wind speeds over the range 2–12 m s^{-1}, is 1.65 m s^{-1}.

CYGNSS MISSION DESCRIPTION. The CYGNSS constellation is composed of eight observatories, evenly spaced about a common orbit plane at 510-km altitude and 35° inclination angle. Each observatory contains a delay Doppler mapping instrument (DDMI) that consists of a multichannel GNSS-R receiver, a low-gain zenith antenna for reception of the direct signals, and two high-gain nadir antennas for reception of the surface scattered signals (Rose et al. 2012; Ruf et al. 2012). There are typically many specular reflections from the surface available at any given time because of the large number of GPS-transmitting satellites. Each DDMI selects the four specular reflections located in the highest sensitivity region of its nadir antenna pattern and simultaneously computes DDMs centered on each of

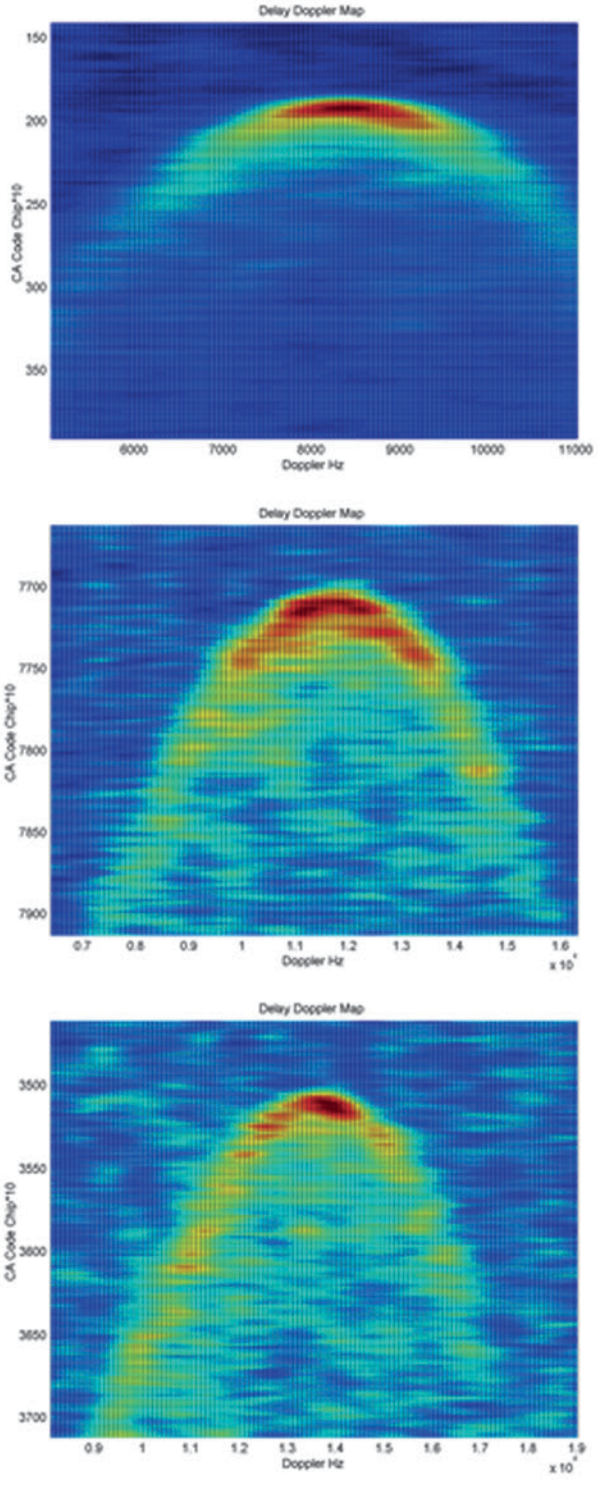

Fig. 3. DDMs of scattered power from the ocean surface as measured by the UK-DMC GNSS-R bistatic radar receiver during NDBC buoy overpasses for three wind speed conditions: (top) 2, (middle) 7, and (bottom) 10 m s^{-1}. The highest power occurs at the specular reflection point (the top of the horseshoe-shaped arc). Diffuse scattered power, away from the specular point, increases as the ocean surface roughness increases due to strengthening winds (Gleason 2006).

them. Individual DDM integration times last 1 s and wind speeds are derived from measurements over a 25 × 25 km^2 region centered on the specular point. This results in a total of 32 wind measurements per second by the full constellation. CYGNSS spatial sampling consists of 32 simultaneous single pixel "swaths" that are 25 km wide and, typically, hundreds of kilometers long, as the specular points move across the surface owing to orbital motion by CYGNSS and the GPS satellites. This sampling process is illustrated by an animation available online (http://dx.doi.org/10.1175/BAMS-D-14-00218.2). Examples of the spatial coverage obtained after 90 min (one orbit) and 24 h are shown in the top and middle panels of Fig. 4. Temporal sampling occurs randomly owing to the asynchronous nature of the CYGNSS and GPS satellite orbits. As a result, the CYGNSS revisit time is best described by its probability distribution. The distribution, shown in the bottom panel of Fig. 4, is derived empirically using a mission simulator to determine the time and location of each sample within the ±38°-latitude coverage zone and then examining the time difference between samples at the same location. The empirical distribution features a high probability of very short revisit times (e.g., resulting from sequential samples by trailing satellites spaced tens of minutes apart) and a long tapering "tail" at higher revisit times. Its median value is 2.8 h and the mean revisit time is 7.2 h.

Wind speed retrieval algorithm. The baseline wind speed retrieval algorithm planned for CYGNSS is an extension of one previously developed for the UK-DMC spaceborne mission, as described in Clarizia et al. (2014) and summarized in the section "Spaceborne demonstration of ocean surface wind retrieval by GNSS-R ." The algorithm uses an empirically derived geophysical model function to estimate the 10-m referenced wind speed from the measured DDM within a 25 × 25 km^2 region centered on the specular reflection point. The UK-DMC algorithm has been extended to higher wind speeds by applying a detailed end-to-end simulator of the CYGNSS measurements to a realistic nature run simulation of the full life cycle of a category-4 hurricane (Nolan et al. 2013). The end-to-end simulator models the complete bistatic radar measurement process, including electromagnetic propagation down from the GPS satellite to the ocean surface, rough surface scattering by the ocean, propagation back up to the CYGNSS satellite, and the engineering design of the CYGNSS GNSS-R receiver (O'Brien 2014). A large population of simulated DDMs, covering a wide dynamic range

of wind speeds, is generated and used to extend the geophysical model function from the lower wind speed regime experienced by UK-DMC to the much higher winds of interest to CYGNSS. The RMS wind speed retrieval error is expected to meet or exceed the mission requirement of 2 m s^{-1} or 10% of the wind speed, whichever is greater.

Postlaunch calibration and validation plans. The primary objectives of the calibration and validation effort are to characterize the geophysical model function, evaluate the performance of each sensor, evaluate the retrieval algorithm, and evaluate the retrieved wind speeds. The first step in this process is collocating various "truth" data with the CYGNSS data. These truth data include numerical model output parameters, GPS dropsondes, other satellite data [e.g., Advanced Scatterometer (ASCAT), *Ocean Satellite (Oceansat)-2* Scatterometer (OSCAT), wind-measuring satellite system (WindSat), Advanced Microwave Scanning Radiometer-2 (AMSR2)], and aircraft-based measurements. The next steps involve statistical analyses of the collocation database. The geophysical model function is characterized and any unexpected artifacts or trends are analyzed. The collocation database is also used to evaluate measurement performance relative to the instrument characteristics and measurement geometry for each sensor. The wind speed retrieval algorithm is analyzed and its strengths and weaknesses are characterized. Quality control flags are developed based on these analyses to be included with the final product files provided to the end users. Another facet of the wind speed retrieval validation will be in the

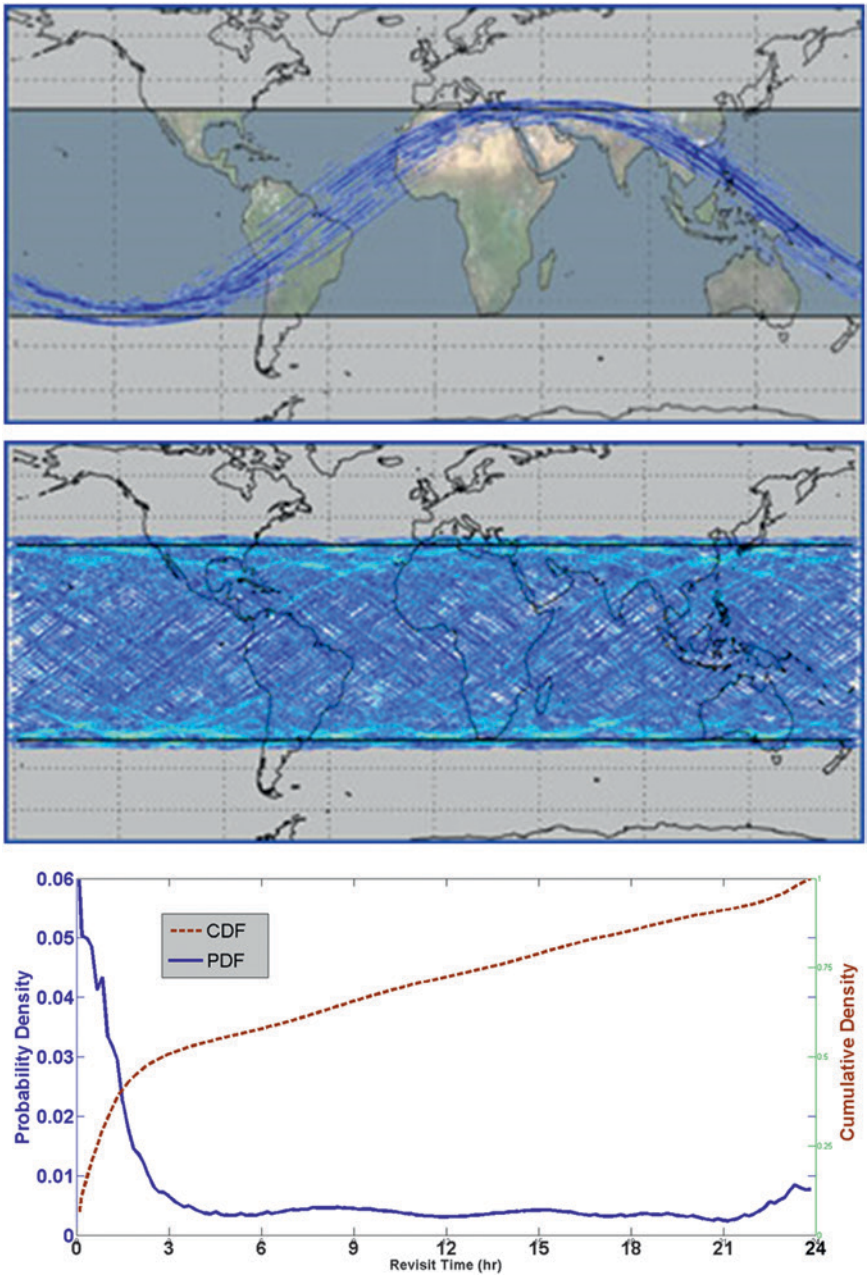

Fig. 4. Each LEO CYGNSS observatory will orbit at an inclination of 35° and be capable of measuring four simultaneous reflections, resulting in 32 wind measurements per second across the globe. The configuration is optimized allowing for high-temporal-resolution wind field imagery of TC genesis, intensification, and decay. Shown here are the CYGNSS spatial coverage tracks after (top) 90 min and (middle) 24 h. (bottom) Temporal sampling is characterized by the probability and cumulative density functions of revisit time. Sampling occurs randomly because of the asynchronous nature of the CYGNSS and GPS satellite orbits, and revisit time is best characterized via statistics of these distributions. The median and mean revisit times are 2.8 and 7.2 h, respectively.

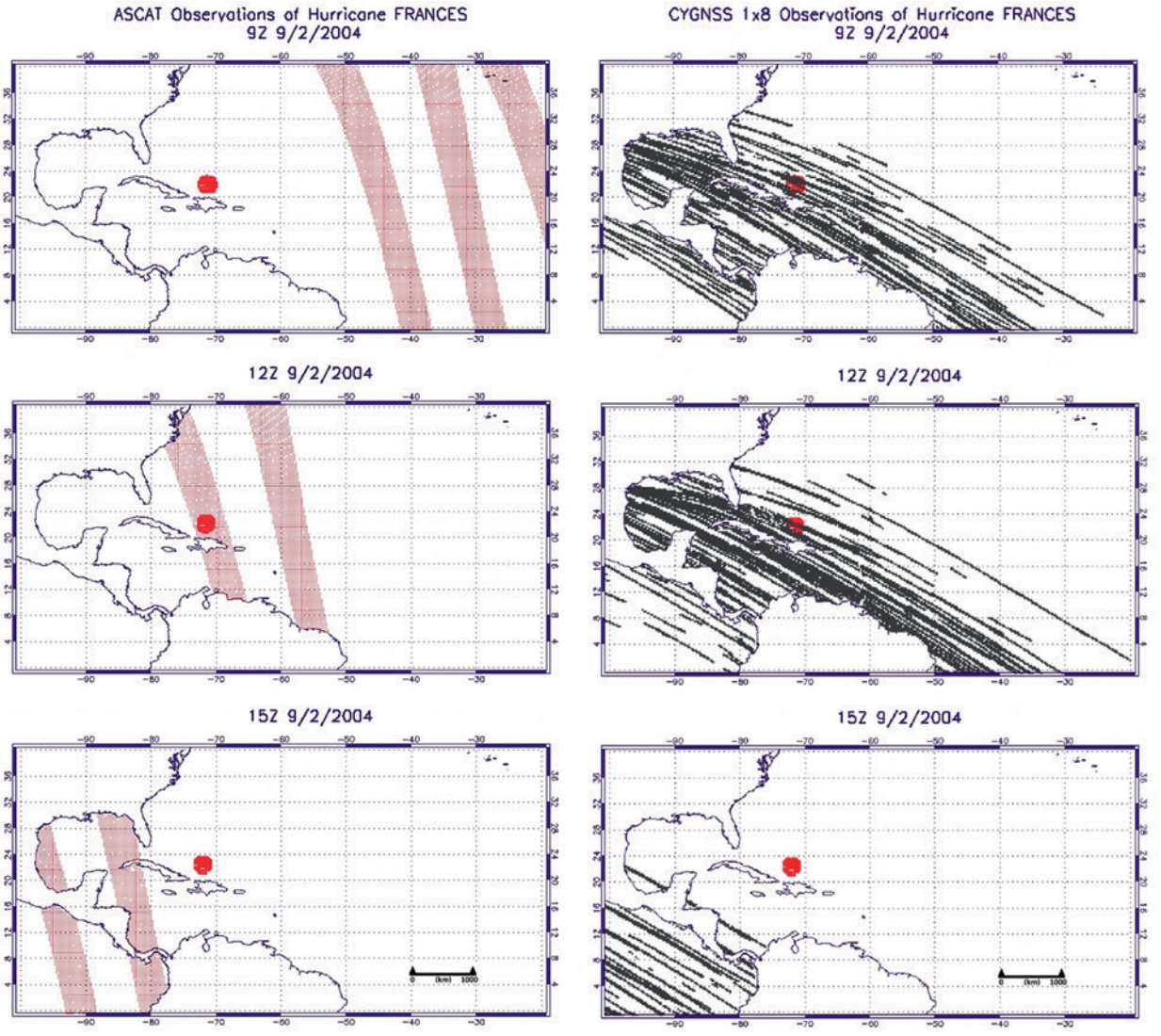

Fig. 5. Time-lapse simulation comparing the spatial and temporal sampling properties of CYGNSS and ASCAT if they had both been in orbit during the Hurricane Frances U.S. landfall on 2 Sep 2004 (Ruf et al. 2012). Each row shows all samples made over successive 3-h intervals and by (left) ASCAT and (right) CYGNSS. The red dot, centered on the storm center and with a 75-km radius, represents the inner-core region. ASCAT swaths are separated by about 1000 km and progress from east to west over time. Only one of the swaths passes over the inner core during the 9-h interval shown. CYGNSS transects are distributed more widely and thus sample in and near the inner core more often.

context of the operational forecasting environment and evaluation of the CYGNSS wind speed product performance by marine forecasters. This type of validation has proven to be invaluable for other satellite data in revealing performance characteristics that are not readily apparent from standard statistical analysis.

There also exists the possibility of directing some under flights of CYGNSS in hurricanes with the NOAA P-3 aircraft for some additional direct comparison datasets at high wind speeds and in limiting environmental conditions. Being the first space-based GNSS-R constellation system that will systematically provide wind speed retrievals over much of the world's oceans, CYGNSS will provide a unique opportunity to characterize and understand the performance of the GNSS-R measurement technique for ocean surface wind speeds.

Another facet of the validation effort will include engaging the operational forecasters at the NOAA National Hurricane Center (NHC). Following each Atlantic hurricane season after launch, the CYGNSS wind retrievals, along with proper training data, will be provided to forecasters to utilize and

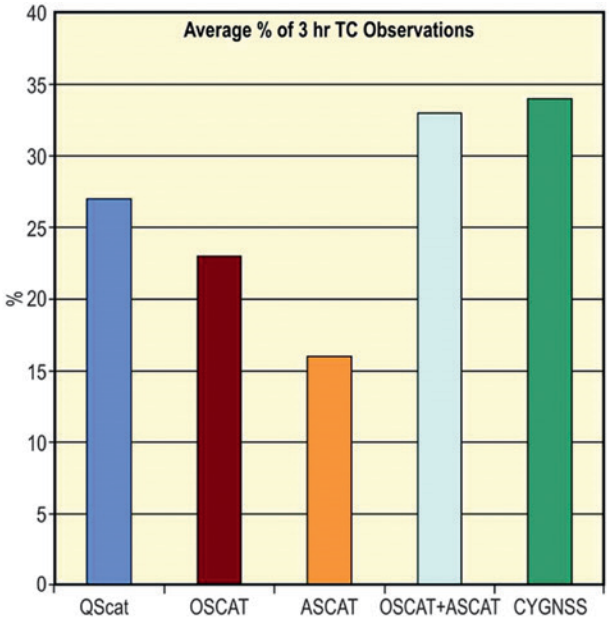

Fig. 6. TC sampling capability as percentage of 3-h intervals in which each sensor measures the TC inner core.

evaluate during their postseason storm analyses. Should CYGNSS data become available in near–real time, an effort will be made to integrate these data into the NHC workstation environment so that they can be utilized and evaluated in near–real time.

Constellation sampling example 1 (resolving TC landfall). A time-lapse simulation comparing CYGNSS and ASCAT coverage of Hurricane Frances (2004) just before its Florida coast landfall is shown in Fig. 5. The simulation was created by projecting satellite coverage predictions for both missions onto the archival storm-track record for Frances. Each frame represents all samples taken within a 3-h interval. The TC inner core is shown as a red-filled circle in each frame. ASCAT, with its relatively narrow swath width, only infrequently samples the inner core, whereas the wider and more dispersed effective swath of the CYGNSS constellation allows for much more frequent sampling (Ruf et al. 2012).

Constellation sampling statistics—Resolving TC life cycle. The simulation used to examine temporal and spatial sampling properties during the Hurricane Frances landfall was extended to the entire 2005 Atlantic hurricane season in a second simulation. In this case, in addition to CYGNSS sampling properties, the sampling by three ocean wind scatterometers [QuikSCAT on NASA SeaWinds, OSCAT on the Indian Space Research Organisation's (ISRO) *OceanSat-2*, and ASCAT on the European Organisation for the Exploitation of Meteorological Satellites's (EUMETSAT) Meteorological Operational (MetOp)] was also modeled. Figure 6 shows the percentage of 3-h intervals over the full hurricane season within which each of the three scatterometers would have sampled the inner-core region of every TC that occurred that year. Also included in the figure is the percentage sampled by the combined OSCAT-and-ASCAT constellation and the percentage that would have been sampled by CYGNSS. CYGNSS has a significantly higher sampling percentage than any single scatterometer and is comparable to the OSCAT-and-ASCAT combination.

Constellation sampling example 2 (wind speed observations). The ability of CYGNSS to resolve the complete wind field of a TC, both the surrounding environmental field and that of the inner core, is illustrated in Fig. 7. Shown is an example of the simulated wind speed measurements made by CYGNSS over a particular 6-h interval in the vicinity of the storm center of the nature run described in Nolan et al. (2013). The spatial sampling is characterized by a large number of interleaved transects along which the winds are measured. They are formed by the trajectories across the ocean surface of the 32 simultaneous specular reflection points being tracked by the CYGNSS constellation. At each reflection point, CYGNSS will measure a DDM and, from it, estimate the wind speed there. The complete time-dependent simulated sampling over the full 13-day life cycle of this nature run is illustrated by an animation available online

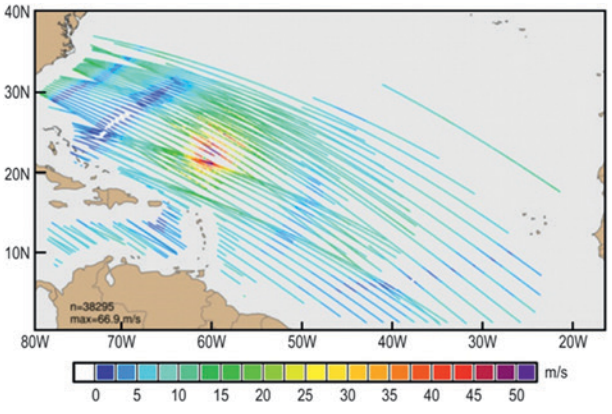

Fig. 7. Simulated wind speeds retrieved by the CYGNSS constellation over a typical 6-h interval in the vicinity of the storm center of the nature run. The simulation includes the effects of all engineering measurement uncertainties as well as the retrieval error associated with the wind speed estimation algorithm. The spatial sampling characteristic of CYGNSS is composed of many interleaved transects formed by the trajectories of the specular reflection points.

Table 1. CYGNSS mission scientific data product baseline requirements.	
Requirement	**Value**
Wind speed dynamic range	3–70 m s^{-1} as determined by a spatially averaged wind field with 5 × 5 km^2 resolution
Wind speed uncertainty	2 m s^{-1} retrieval uncertainty for winds less than 20 m s^{-1} 10% retrieval uncertainty for winds greater than 20 m s^{-1}
Precipitation tolerance	Meet dynamic range and uncertainty requirements at rain rates of up to 100 mm h^{-1} as determined by a spatially averaged rain field with 5 × 5 km^2 resolution
Spatial resolution	25 × 25 km^2 or better
Mean revisit time	Less than 12 h
24-h spatial coverage	70% or more of the TC historical tracks

(http://dx.doi.org/10.1175/BAMS-D-14-00218.2). In the animation, measurements made by each of the eight individual spacecraft are distinguished by unique icons. The wind speeds shown in Fig. 7 are those retrieved by CYGNSS and include the effects of expected engineering measurement uncertainties as well as errors associated with the wind speed retrieval algorithm. These results are currently being used in assimilation studies to assess their impact on hurricane intensity and track forecasts.

CONCLUSIONS. The CYGNSS mission is scheduled for launch in October 2016. Its use of multichannel GNSS-R bistatic radar scatterometers, flown on a constellation of eight satellites in a low-inclination orbit, results in a unique ability to measure ocean surface winds in the inner core of tropical cyclones with a revisit time of hours. A summary of the mission's science measurement requirements is listed in Table 1. It is hoped and expected that this unique dataset will contribute to significant improvements in our understanding of TC inner-core processes and in our ability to model and forecast their development.

ACKNOWLEDGMENTS. The work presented was supported in part by NASA Science Mission Directorate Contract NNL13AQ00C. The authors would also like to thank Dave Nolan for providing the nature run simulation data and Brian McNoldy for producing the spatial sampling image (Fig 7).

REFERENCES

Arguez, A., M. A. Bourassa, and J. J. O'Brien, 2005: Detection of the MJO signal from QuikSCAT. *J. Atmos. Oceanic Technol.*, **22**, 1885–1894, doi:10.1175/JTECH1822.1.

Atlas, R., and Coauthors, 2001: The effects of marine winds from scatterometer data on weather analysis and forecasting. *Bull. Amer. Meteor. Soc.*, **82**, 1965–1990, doi:10.1175/1520-0477(2001)082<1965:TEOMWF>2.3.CO;2.

——, A. Y. Hou, and O. Reale, 2005a: Application of SeaWinds scatterometer and TMI-SSM/I rain rates to hurricane analysis and forecasting. *J. Photogramm. Remote Sens.*, **59**, 233–243, doi:10.1016/j.isprsjprs.2005.02.007.

——, and Coauthors, 2005b: Hurricane forecasting with the high-resolution NASA finite volume general circulation model. *Geophys. Res. Lett.*, **32**, L03807, doi:10.1029/2004GL021513.

Brown, D. P., and J. L. Franklin, 2004: Dvorak TC wind speed biases determined from reconnaissance-based "best track" data (1997–2003). *26th Conf. on Hurricanes and Tropical Meteorology*, Miami, FL, Amer. Meteor. Soc., 3D.5. [Available online at https://ams.confex.com/ams/26HURR/techprogram/paper_75193.htm.]

Clarizia, M. P., C. Gommenginger, S. Gleason, M. Srokosz, C. Galdi, and M. di Bisceglie, 2009: Analysis of GNSS-R delay-Doppler maps from the UK-DMC satellite over the ocean. *Geophys. Res. Lett.*, **36**, L02608, doi:10.1029/2008GL036292.

——, C. Ruf, C. Gommenginger, and P. Jales, 2014: Spaceborne GNSS-R minimum variance wind speed estimator. *IEEE Trans. Geosci. Remote Sens.*, **52**, 6829–6843, doi:10.1109/TGRS.2014.2303831.

Gall, R., J. Franklin, F. Marks, E. N. Rappaport, and F. Toepfer, 2013: The Hurricane Forecast Improvement Project. *Bull. Amer. Meteor. Soc.*, **94**, 329–343, doi:10.1175/BAMS-D-12-00071.1.

Garrison, J., S. Katzberg, and M. Hill, 1998: Effect of sea roughness on bistatically scattered range coded signals from the global positioning system. *Geophys. Res. Lett.*, **25** , 2257–2260, doi:10.1029/98GL51615.

——, A. Komjathy, V. Zavorotny, and S. J. Katzberg, 2002: Wind speed measurements using forward scattered GPS signals. *IEEE Trans. Geosci. Remote Sens.*, **40**, 50–65, doi:10.1109/36.981349.

Gleason, S., 2006: Remote sensing of ocean, ice and land remote sensing using bistatically scattered GNSS signals from low earth orbit. Ph.D. thesis, University of Surrey, 223 pp.

——, 2013: Space-based GNSS scatterometry: Ocean wind sensing using an empirically calibrated model. *IEEE Trans. Geosci. Remote Sens.*, **51**, 4853–4863, doi:10.1109/TGRS.2012.2230401.

——, S. Hodgart, S. Yiping, C. Gommenginger, S. Mackin, M. Adjrad, and M. Unwin, 2005: Detection and processing of bistatically reflected GPS signals from low Earth orbit for the purpose of ocean remote sensing. *IEEE Trans. Geosci. Remote Sens.*, **43**, 1229–1241, doi:10.1109/TGRS.2005.845643.

——, C. Gommenginger, and D. Cromwell, 2010: Fading statistics and sensing accuracy of ocean scattered GNSS and altimetry signals. *J. Adv. Space Res.*, **46**, 208–220, doi:10.1016/j.asr.2010.03.023.

Houze, R. A., Jr., 2004: Mesoscale convective systems. *Rev. Geophys.*, **42**, RG4003, doi:10.1029/2004RG000150.

Katzberg, S. J., and J. Dunion, 2009: Comparison of reflected GPS wind speed retrievals with dropsondes in tropical cyclones. *Geophys. Res. Lett.*, **36**, L17602, doi:10.1029/2009GL039512.

——, R. A. Walker, J. H. Roles, T. Lynch, and P. G. Black, 2001: First GPS signals reflected from the interior of a tropical storm: Preliminary results from Hurricane Michael. *Geophys. Res. Lett.*, **28**, 1981–1984, doi:10.1029/2000GL012823.

——, O. Torres and G. Ganoe, 2006: Calibration of reflected GPS for tropical storm wind speed retrievals. *Geophys. Res. Lett.*, **33**, L18602, doi:10.1029/2006GL026825.

Lin, B., S. J. Katzberg, J. L. Garrison, and B. Wielicki, 1998: Relationship between the GPS signals reflected from sea surface and the surface winds: Modeling results and comparisons with aircraft measurements. *J. Geophys. Res.*, **104**, 20713–20727, doi:10.1029/1999JC900176.

Lowe, S. T., J. L. LaBrecque, C. Zuffada, L. Romans, L. Young, and G. Hajj, 2002: First spaceborne observation of an Earth-reflected GPS signal. *Radio Sci.*, **37**, 7-1–7-28, doi:10.1029/2000RS002539.

Nesbitt, S. W., E. J. Zipser, and D. J. Cecil, 2000: A census of precipitation features in the Tropics using TRMM: Radar, ice scattering, and lightning observations. *J. Climate*, **13**, 4087–4106, doi:10.1175/1520-0442(2000)013<4087:ACOPFI>2.0.CO;2.

Nolan, D. S., R. Atlas, K. T. Bhatia, and L. R. Bucci, 2013: Development and validation of a hurricane nature run using the Joint OSSE nature run and the WRF model. *J. Adv. Earth. Model. Syst.*, **5**, 382–405, doi:10.1002/jame.20031.

O'Brien, A., 2014: End-to-end simulator. CYGNSS Project, Space Physics Research Laboratory Doc. 148-0123, University of Michigan, 24 pp.

Rickenbach, T. M., and S. A. Rutledge, 1998: Convection in TOGA COARE: Horizontal scale, morphology, and rainfall production. *J. Atmos. Sci.*, **55**, 2715–2729, doi:10.1175/1520-0469(1998)055<2715:CITCHS>2.0.CO;2.

Rose, R., J. Dickinson, and A. Ridley, 2012: CubeSats to NanoSats; Bridging the gap between educational tools and science workhorses. *2012 IEEE Aerospace Conf.*, Big Sky, MT, IEEE, doi:10.1109/AERO.2012.6187417.

Ruf, C. S., S. Gleason, Z. Jelenak, S. Katzberg, A. Ridley, R. Rose, J. Scherrer, and V. Zavorotny, 2012: The CYGNSS nanosatellite constellation hurricane mission. *2012 IEEE Int. Geoscience and Remote Sensing Symp.*, Munich, Germany, IEEE, 214–214, doi:10.1109/IGARSS.2012.6351600.

Schlax, M. G., D. B. Chelton, and M. H. Freilich, 2001: Sampling errors in wind fields constructed from single and tandem scatterometer datasets. *J. Atmos. Oceanic Technol.*, **18**, 1014–1036, doi:10.1175/1520-0426(2001)018<1014:SEIWFC>2.0.CO;2.

Stephens, G. L., P. J. Webster, R. H. Johnson, R. Engelen, and T. L'Ecuyer, 2004: Observational evidence for the mutual regulation of the tropical hydrological cycle and tropical sea surface temperatures. *J. Climate*, **17**, 2213–2224, doi:10.1175/1520-0442(2004)017<2213:OEFTMR>2.0.CO;2.

Zavorotny, V., and A. Voronovich, 2000: Scattering of GPS signals from the ocean with wind remote sensing applications. *IEEE Trans. Geosci. Remote Sens.*, **38**, 951–964, doi:10.1109/36.841977.